

NUMERICAL SIMULATIONS OF INERTIA FLOWS OF REGULARIZED BINGHAM FLUIDS VIA A MIXED STABILIZED FORMULATION OF FINITE ELEMENTS

Filipe de Santis Silveira, fsilveira@mecanica.ufrgs.br

Sergio Frey¹, frey@mecanica.ufrgs.br

Laboratory of Applied and Computational Fluid Mechanics (LAMAC)
Mechanical Engineering Department, UFRGS
Rua Sarmiento Leite, 425 – 90059-170 – Porto Alegre, RS, Brazil.

Flávia Zinani, fzinani@unisinis.br

Mechanical Engineering Department
UNISINOS – Universidade do Vale do Rio dos Sinos
Av. Unisinis, 950 – 93.022-000 – São Leopoldo, RS, Brazil

Abstract. *In this article, numerical approximations of linear viscoplastic fluid flows have been considered in order to investigate the yield surface morphology in viscoplastic materials flowing subjected to inertia effects. Viscoplastic material equations model the behavior of some structured liquids that present deep changes in their mechanical properties within a small stress range, and no-flow conditions prevail at low stress levels. Here, the selected viscoplastic equation has been the well-known Bingham model regularized by the Papanastasiou strategy. The employed mechanical model has consisted of the Bingham equation coupled with continuity and motion equations. This model has been approximated by a stabilized finite element formulation - namely a Galerkin-least-squares-like methodology - that aims to enhance the classical Galerkin stability without upsetting its consistency. Some two-dimensional numerical simulations have been investigated employing the lid-driven cavity flow. In the studied flows, the influence of inertia and shear stress have been evaluated, with the values of Reynolds and Bingham numbers considered for significant ranges of interest. In all computations, a combination of Lagrangian bilinear equal-order interpolations for velocity and pressure fields has been used - a choice a priori interdicted by the Babuška-Brezzi compatibility condition. The numerical results have allowed to verify the accuracy and stability of the employed stabilized formulation and were matched with classical results of viscoplastic literature.*

Keywords: *Viscoplastic materials; classical Bingham model; Papanastasiou regularization; mixed stabilized formulation; Galerkin least-squares methodology.*

1. INTRODUCTION

The Bingham constitutive model was built to describe the behavior of a viscoplastic material, which flows as Newtonian fluid when its shear stress level exceeds the yield limit. However, the classical Bingham model, as originally proposed (Bird et al, 1983), suffers from a serious shortcoming: in this model, the shear stress is a non-smooth field and two distinct equations are needed to describe both unyielded and yielded regions.

In order to circumvent this drawback, enlarging in this way the applicability of the Bingham model to a wider class of real viscoplastic materials, Papanastasiou (1987) has proposed a regularizing strategy that describes the shear stress field on the whole shear rate domain by a single equation. In this equation, the yield stress term of the classical Bingham model is multiplied by a regularizing term, which controls the yield stress exponential decay. In doing so, the regularized Bingham model is able to well predict the viscoplastic behavior of a large class real materials which present high finite viscosity values for very small strain rates.

This work aims to perform finite element approximations for inertia flows of regularized Bingham fluids employing a mixed stabilized formulation based on the Galerkin least-squares (GLS) methodology. The stabilized formulation circumvents the well-known Babuška-Brezzi condition (see Babuška, 1973 and Brezzi, 1974) – hence admitting any combination of velocity and pressure interpolations – and adds artificial diffusivity, in a selective way, to diffusive and advective dominated regions of the flow – the latter, a very useful feature when handling with fluids subjected to shear-thinning effects and materials presenting yield stress. The considered geometry has been the classical benchmark of the lid driven cavity. The computations have investigated how the yield stress limit and the inertia effects have influenced the yielded surface morphology and the viscoplastic flow dynamics. For that, the Bingham number has been varied from 1 up to 1000 and the Reynolds number from 0 to 1000. The obtained numerical results have remained stable even for an equal-order combination of velocity and pressure interpolations and high values of Reynolds and Bingham numbers. Besides, the results have been in accordance with the viscoplastic literature.

¹ Corresponding author.

2. MECHANICAL MODELING

The mechanical model considered in this article employs the continuity and motion equations, for isothermal incompressible flows, coupled with a material equation for viscoplastic liquids.

2.1. Mass conservation

The principle of mass conservation of a mechanical body states that the rate of increase of the fluid mass within a bounded fluid volume Ω is equal to the net afflux of fluid across the its surface Γ . Applying the Gauss and Reynolds transport theorems (Slattery (1999)) and exploiting the arbitrariness of Ω , this principle may be expressed, in Cartesian index notation, as

$$\partial_t \rho + \partial_{x_i} (\rho u_i) = 0 \quad (1)$$

where ρ is the mass density of the fluid and u_i the i -component of velocity field.

2.2. Momentum balance

According to the law of momentum balance, the rate of increase of momentum of the fluid volume Ω is equal to the net flow of momentum into Ω added to the sum of all surface and body forces acting on Ω . Applying the hypothesis used in Eq. (1), one may obtain (Slattery (1999))

$$\partial_t (\rho u_i) = -\partial_{x_j} (\rho u_i u_j) + \partial_{x_j} T_{ij} + \rho f_i, \text{ for } i=1, N \quad (2)$$

where T_{ij} the ij -component of the stress tensor, ρf_i the i -component of the body forces acting on Ω , N the number of space dimensions and the reminding variables are defined as previously. Next, imposing the fluid incompressibility assumption, the *Eulerian form of motion equation* may be achieved,

$$\rho (\partial_t u_i + u_j \partial_{x_j} u_i) = \partial_{x_j} T_{ij} + \rho f_i, \text{ for } i=1, N \quad (3)$$

2.3. Constitutive relations

In this article, the generalized Newtonian constitutive equation (GNL) has been assumed to relate the internal stresses to flow kinematic variables (Bird et al, 1983),

$$T_{ij} = -p 1_{ij} + \tau_{ij} = -p 1_{ij} + 2 \eta(\dot{\gamma}) D(u)_{ij}, \text{ for } i, j=1, N \quad (4)$$

where p is a mean pressure for incompressible fluids, $p \equiv -1/3 T_{ii}$, 1_{ij} the unity tensor, and τ_{ij} the extra-stress tensor and $D_{ij} = 1/2 (\partial_{x_j} u_i + \partial_{x_i} u_j)$ is the rate of strain tensor, whose magnitudes are respectively given by

$$\tau = (1/2 \tau_{ij} \tau_{ij})^{1/2} \text{ and } \dot{\gamma} = (2 D(u)_{ij} D(u)_{ij})^{1/2} \quad (5)$$

In addition, $\eta(\dot{\gamma}) \equiv \tau / \dot{\gamma}$ is the GNL viscosity function, (Bird et al, 1983).

In order to model the stress-strain behavior of a viscoplastic material, the Bingham constitutive model have been chosen. This model is characterized by a viscoplastic relation between extra-stress and shear rate, flowing as a constant viscosity fluid when the shear stress exceeds the yield value of the material, τ_0 . For shear stress values below τ_0 , moving or unmoving (dead) unyielded zones are characterized. The classical Bingham model may expressed by (Bird et al., 1983):

$$\begin{aligned} \tau &= \tau_0 + \eta_p \dot{\gamma} & \text{for } \tau \geq \tau_0 \\ \dot{\gamma} &= 0 & \text{for } \tau < \tau_0 \end{aligned} \quad (6)$$

where η_p is the fluid plastic viscosity and τ_0 and $\dot{\gamma}$ and τ are defined as previously.

Papanastasiou (1987) proposed a modification of Eq. (6) by introducing a regularization parameter m , which expresses the shear stress as a continuous function, valid for the whole shear rate domain. The advantage of this

regularization is to eliminate the non-smoothness of the τ field at $\tau=\tau_0$. The resulting regularized equation is valid for both yielded and unyielded zones, giving rise to the following shear stress and viscosity functions, respectively:

$$\tau = \eta_p \dot{\gamma} + \tau_0 [1 - \exp(-m \dot{\gamma})] \quad (7)$$

and

$$\eta(\dot{\gamma}) = \eta_p + \frac{\tau_0}{\dot{\gamma}} [1 - \exp(-m \dot{\gamma})] \quad (8)$$

Eq. (7) states that as $m \rightarrow 0$, the expression for τ reduces to the classical Newtonian model and hence the viscosity function $\eta(\dot{\gamma})$ (Eq. (8)) tends to the Newtonian constant viscosity; otherwise, as $m \rightarrow \infty$, Eq. (7) mimics the classical Bingham model and Eq. (8) the classical Bingham viscosity function – as illustrated in Fig. 1.

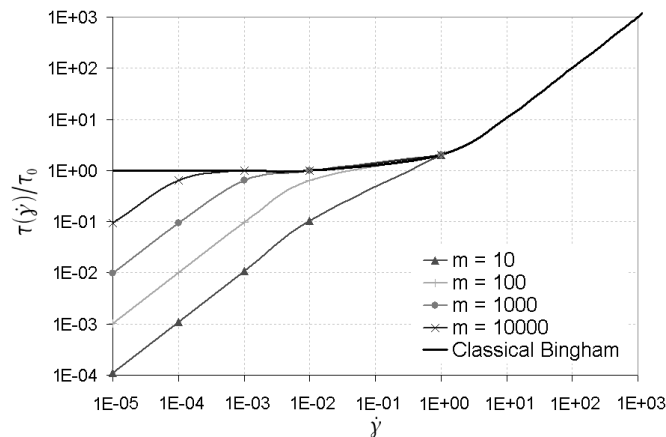


Figure 1. Shear stress vs. strain rate curves, for some values of the Papanastasiou regularizing parameter m .

3. FINITE ELEMENT APPROXIMATION

Taking into account the mass and momentum governing equations, Eq. (1) and (3) respectively, for an inelastic incompressible fluid on steady-state flow, coupled with the regularized Bingham viscosity function, Eq. (8), the following boundary value problem may be stated,

$$\begin{aligned} \rho(u_j \partial_{x_j} u_i) + \partial_{x_i} p - 2(\eta_p + \frac{\tau_0}{\dot{\gamma}} [1 - \exp(-m(2 D(u)_{op} D(u)_{op})^{1/2})]) \partial_{x_j} D(u)_{ij} \\ - D(u)_{ij} \partial_{x_j} (2(\eta_p + \frac{\tau_0}{\dot{\gamma}} [1 - \exp(-m(2 D(u)_{op} D(u)_{op})^{1/2})])) = f_i \quad \text{in } \Omega, \text{ for } i=1, N \\ \partial_{x_i} u_i = 0 \quad \text{in } \Omega \\ u_i = u_{g_i} \quad \text{on } \Gamma_{g_i}, \text{ for } i=1, N \\ (-p I_{ij} + 2(\eta_p + \frac{\tau_0}{\dot{\gamma}} [1 - \exp(-m(2 D(u)_{op} D(u)_{op})^{1/2})]) D(u)_{ij}) n_j = t_{h_i} \quad \text{on } \Gamma_{h_i}, \text{ for } i=1, N \end{aligned} \quad (9)$$

where Ω represents the flow domain, Γ_{g_i} and Γ_{h_i} the boundary portions on which Dirichlet velocity conditions and Neumann stress conditions are respectively imposed, \mathbf{u}_{g_i} the prescribed velocity and the field \mathbf{t}_{h_i} the stress vector. The remaining variables have been previously defined.

The stabilized finite element method was built in employing an conforming approximation for the finite element subspaces for velocity (V^h) and pressure (P^h),

$$\begin{aligned} V_i^h &= \{v_i \in H_0^1(\Omega) | v_{i_k} \in R_k(K), K \in \Omega^h\} \\ P^h &= \{q \in C^0(\Omega) \cap L_0^2(\Omega) | q_K \in R_i(K), K \in \Omega^h\} \\ V_{g_i}^h &= \{v_i \in H^1(\Omega) | v_{i_k} \in R_k(K), K \in \Omega^h, v_i = u_{g_i} \text{ on } \Gamma_{g_i}\} \end{aligned} \quad (10)$$

with $C^0(W)$ representing the space of continuous functions, $L^2(\Omega)$ the Hilbert space of square integrable functions in Ω , $H^1(\Omega)$ the Sobolev functional space of functions with square integrable value and derivatives in Ω (see, for instance, Rektorys (1973) for definition of infinite dimension spaces), R_k and R_l the polynomial of degrees k and l in Ω^h (Ciarlet, 1978) and N represents the number of space dimensions considered in the problem.

3.1. A Mixed stabilized formulation

A mixed stabilized formulation, based on the Galerkin least-squares methodology (Franca and Frey (1992)), for the boundary-value problem defined by Eq. (9) may be stated as: given $f_i: \Omega \rightarrow \mathfrak{R}$, $u_{g_i}: \Gamma_{g_i} \rightarrow \mathfrak{R}$, $t_{h_i}: \Gamma_{h_i} \rightarrow \mathfrak{R}$, for $i=1, \dots, N$, and the pair $(u_i^h, p^h) \in V_{g_i}^h \times P^h$, for $i=1, \dots, N$, such that:

$$B(u_i^h, p^h; v_i^h, q^h) = F(v_i^h, q^h), \quad \forall (v_i^h, q^h) \in V_i^h \times P^h \quad (11)$$

with

$$\begin{aligned} B(u_i^h, p^h; v_i^h, q^h) = & \int_{\Omega} \rho(u_j^h \partial_{x_j} u_i^h) v_i^h d\Omega + \int_{\Omega} 2(\eta_p + \frac{\tau_0}{\dot{\gamma}} [1 - \exp(-m(2 D(u)_{op} D(u)_{op})^{1/2})]) D(u^h)_{ij} D(v^h)_{ij} d\Omega \\ & - \int_{\Omega} 2D(u^h)_{ij} \partial_{x_j} (\eta_p + \frac{\tau_0}{\dot{\gamma}} [1 - \exp(-m(2 D(u)_{op} D(u)_{op})^{1/2})]) v_i^h d\Omega - \int_{\Omega} p^h \partial_{x_i} v_i^h d\Omega - \int_{\Omega} \partial_{x_i} u_i^h q^h d\Omega \\ & + \varepsilon \int_{\Omega} p^h q^h d\Omega + \sum_{K \in \Omega^h} \int_{\Omega_K} (\rho(u_j^h \partial_{x_j} u_i^h) + \partial_{x_i} p^h - 2(\eta_p + \frac{\tau_0}{\dot{\gamma}} [1 - \exp(-m(2 D(u)_{op} D(u)_{op})^{1/2})]) \partial_{x_j} D(u^h)_{ij} \\ & \quad - 2D(u^h)_{ij} \partial_{x_j} (\eta_p + \frac{\tau_0}{\dot{\gamma}} [1 - \exp(-m(2 D(u)_{op} D(u)_{op})^{1/2})])) \\ & \quad \alpha(\text{Re}_K)(\rho(u_j^h \partial_{x_j} v_i^h) - \partial_{x_i} q^h + 2(\eta_p + \frac{\tau_0}{\dot{\gamma}} [1 - \exp(-m(2 D(u)_{op} D(u)_{op})^{1/2})]) \partial_{x_j} D(v^h)_{ij} \\ & \quad + 2D(v^h)_{ij} \partial_{x_j} (\eta_p + \frac{\tau_0}{\dot{\gamma}} [1 - \exp(-m(2 D(u)_{op} D(u)_{op})^{1/2})])) d\Omega \end{aligned} \quad (12)$$

and

$$\begin{aligned} F(v_i^h, q^h) = & \int_{\Omega} f_i v_i^h d\Omega + \int_{\Gamma_{h_i}} t_{h_i} v_i^h d\Omega \\ & + \sum_{K \in \Omega^h} \int_{\Omega_K} \alpha(\text{Re}) f_i (\rho(u_j^h \partial_{x_j} v_i^h) - \partial_{x_i} q^h + 2(\eta_p + \frac{\tau_0}{\dot{\gamma}} [1 - \exp(-m(2 D(u)_{op} D(u)_{op})^{1/2})]) \partial_{x_j} D(v^h)_{ij} \\ & \quad + 2D(v^h)_{ij} \partial_{x_j} (\eta_p + \frac{\tau_0}{\dot{\gamma}} [1 - \exp(-m(2 D(u)_{op} D(u)_{op})^{1/2})])) d\Omega \end{aligned} \quad (13)$$

where ε denotes a positive constant, $\varepsilon \ll 1$, and α the GLS stability parameter defined as in Franca and Frey (1992),

$$\begin{aligned} \alpha(\text{Re}_K) = & \frac{h_K}{2(\sum_{i=1}^n u_i^p)^{1/p}} \xi(\text{Re}_K), \quad \text{with } \xi(\text{Re}_K) = \begin{cases} \text{Re}_K, & 0 < \text{Re}_K < 1 \\ 1, & \text{Re}_K > 1 \end{cases} \\ \text{Re}_K = & \frac{\rho m_k (\sum_{i=1}^n u_i^p)^{1/p} h_K}{4(\eta_p + \frac{\tau_0}{\dot{\gamma}} [1 - \exp(-m(1/2 D(u)_{op} D(u)_{op})^{1/2})])}, \quad \text{with } m_k = \min\{1/3, 2C_k\} \\ & \sum_{K \in \Omega^h} h_K^2 \int_{\Omega} \partial_{x_j} (D(v^h)_{ij}) \partial_{x_k} (D(v^h)_{ik}) d\Omega \geq C_k \int_{\Omega} D(v^h)_{ij} D(v^h)_{ij} d\Omega \quad \forall v_i^h \in V_i^h \end{aligned} \quad (14)$$

in which h_K stands for the K -element size, Re_K the grid Reynolds number, $\|\mathbf{u}\|_p$ the p -norm on \mathfrak{R}^N and the other variables defined as previously.

Remark: The employed nonlinear solver for the matrix problem associated to the stabilized formulation defined by Eq. (11)-(14) was a quasi-Newton method with a frozen Jacobian gradient strategy - in which the Jacobian matrix was only updated at two or three Newtonian iterations. Besides, the solver has also used an incremental continuation over the geometrical and material non-linearity, which allowed to achieved high viscoplastic regimen starting from null velocity and pressure fields - see Zinani and Frey (2006) for a detailed description of the complete algorithm.

4. NUMERICAL RESULTS

In this section, mixed stabilized approximations (Eq. (11)-(14)) for inertia flows of regularized Bingham fluids inside a lid driven square cavity have been carried out. The cavity length was $L=1\text{m}$ and its lid velocity u_{lid} was equal to 1m/s – see Fig. 2 for the problem statement. The imposed velocity conditions were impermeability and no-slip at all cavity walls but the lid, where the horizontal uniform velocity u_{lid} has been prescribed.

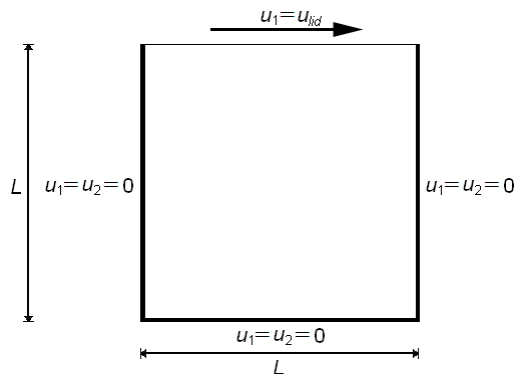


Figure 2. Lid-driven cavity flow: problem statement.

The Bingham and Reynolds number were respectively defined in the usual way. The former one by (Bird *et al.*, 1987),

$$\text{Bn} = \frac{\tau_0}{\eta_c \dot{\gamma}_c} \quad (15)$$

and the Reynolds number as

$$\text{Re} = \frac{\rho U_c L_c}{\eta_c} \quad (16)$$

where the characteristic length L_c , velocity U_c , shear rate $\dot{\gamma}_c$ and viscosity η_c were respectively given by L , u_{lid} , (u_{lid}/L) and η_p , with the latter standing for the fluid plastic viscosity. The Bingham number was ranged for values from 1 to 1000, while the Reynolds number investigated between 0 and 1000. After a mesh independence procedure, a 80×80 Q_1/Q_1 equal-order Lagrangian finite elements have been used and, in all computations, the Papanastasiou regularization parameter m has been fixed as 1000 – as suggested by some viscoplastic researchers (for instance, Mitsoulis and Zisis (2001) and Neofytou (2005)). The numerical simulations were undertaken by a finite element code for non-linear fluids under development at Laboratory of Computational and Applied Fluid Mechanics (LAMAC) of Federal University of Rio Grande do Sul.

In Fig. 3, the yield stress effects on the viscoplastic fluid dynamics have been analyzed, through the plotting of the extra-stress isobands, have been concerned. For inertialess flows, the Bingham number has been investigated for a very wide range of values, varying from $\text{Bn}=1$ to $\text{Bn}=1000$. For low Bingham flows – namely for $\text{Bn}=1$ (Fig. 3a) and $\text{Bn}=5$ (Fig. 3b) – the morphology of unyielded material regions (the black ones, in the figure) has proved to be strongly dependent on the growth of Bingham number, whereas, for high values of Bingham, this dependency seems to weaken, as may be verified for the higher values of Bingham, for $\text{Bn}=20$ (Fig. 3c) and $\text{Bn}=1000$ (Fig. 3d).

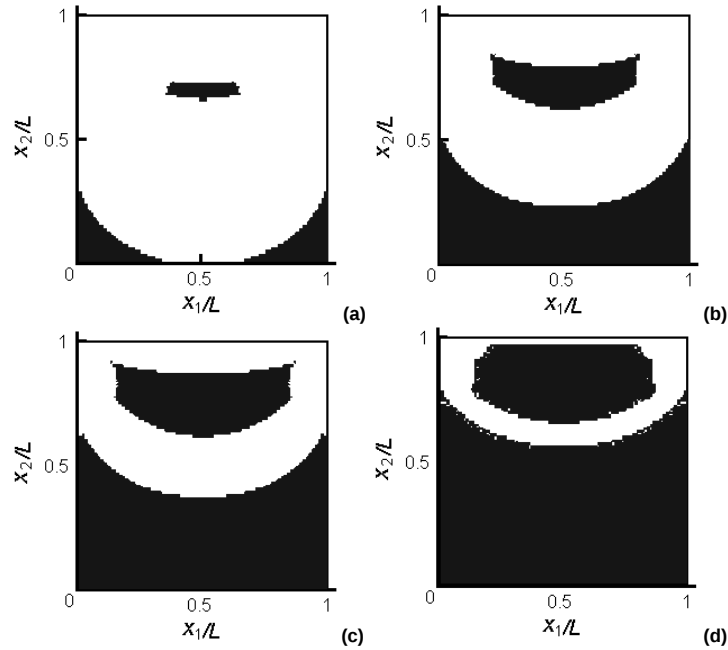


Figure 3. Extra-stress isobands, for $Re=0$: (a) $Bn=1$, (b) $Bn=5$, (c) $Bn=20$, (d) $Bn=1000$.

Aiming to check the stability of the formulation defined by Eq. (11)-(14), for flows subjected to high material non-linearity, the pressure elevation plots related to Bingham number have been plotted in Fig. 4. Undoubtedly, the stabilized formulation has been able to erase the spurious oscillations on the pressure surfaces even for very high Bingham flows ($Bn=1000$, Fig. 4d), employing a combination of equal-order finite element interpolations that violates the Babuška-Brezzi condition.

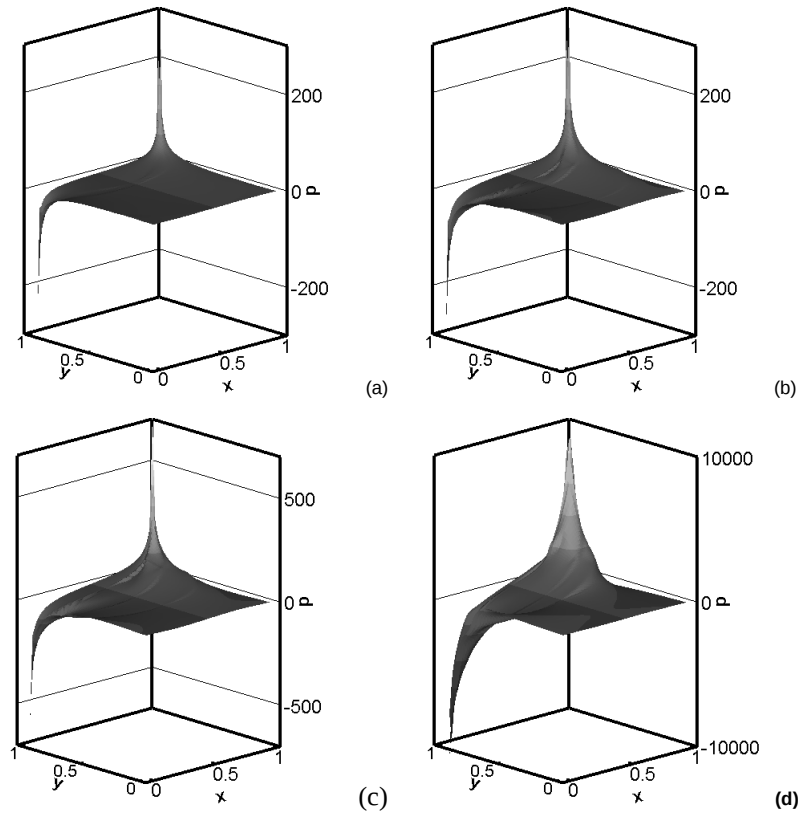


Figure 4. Pressure elevation plots, for $Re=0$: (a) $Bn=1$, (b) $Bn=5$, (c) $Bn=20$, (d) $Bn=1000$.

In order to focus the attention on the yield stress influence in inertia flows, Fig. 5 has shown fluid flow streamlines for a high value of the Reynold number, $Re=1000$, and four distinct values of the Bingham number – namely $Bn=1$ (Fig. 5a), $Bn=2$ (Fig. 5b), $Bn=3$ (Fig. 5c) and $Bn=5$ (Fig. 5d). It may be noticed from the figure that the Bingham number increase has clearly tended to shrink the secondary back-flows at the inferior corners of the cavity. This streamline pattern may be due to crescent role of the viscous effects forced by the increasing of the Bingham number.

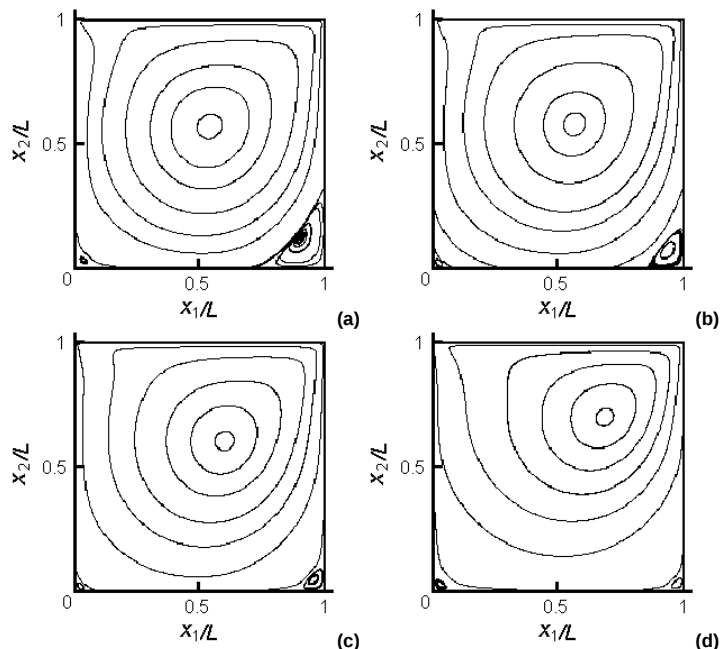


Figure 5. Fluid flow streamlines, for $Re=1000$ and low Bingham regime: (a) $Bn=1$, (b) $Bn=2$, (c) $Bn=3$, (d) $Bn=5$.

5. FINAL REMARKS

In this article, mixed stabilized finite element approximations of Bingham fluid flows regularized by Papanastasiou equation have been performed. The employed stabilized formulation, a Galerkin-least-squares-like methodology, has been able to secure stable approximations even for a pair of equal-order Lagrangian finite element interpolations for velocity and pressure violating the Babuška-Brezzi compatibility condition, and for very high Bingham and Reynolds fluid flows. From the numerical investigation, it may be verified that, for creeping flows, the morphology of the unyielded zones has been strongly influenced by the increasing of the Bingham number, with the same not necessarily occurring for high values of the Bingham number. Besides, still for inertialess flows, the stability of stabilized formulation has been checked, presenting smooth pressure elevation plots. At length, now for inertia flows, it has been shown the shrinking of the secondary vortices at the inferior cavity corners due to the increasing of viscous effects.

6. ACKNOWLEDGEMENTS

The author F. Silveira thanks for its scholarship provided by CNPq and the author S. Frey acknowledges CNPq for financial support.

7. REFERENCES

- Barnes, H.A., 1999, "The Yield Stress – a Review or 'παντα ρει' – Everything Flows?", J. Non-Newtonian Fluid Mech., Vol. 81, pp. 133-178.
- Bird R.B, Armstrong R.C. and Hassager, O., 1987, "Dynamics of polymeric liquids, Vol. 1, Fluid Dynamics". John Wiley and Sons, New York, USA.
- Babuška I., 1973, "The finite element method with Lagrangian multipliers". Vol. 20, pp.179-192.
- Brezzi F., 1974, "On the existence, uniqueness and approximation of saddle-point problems arising from Lagrange multipliers", RAIRO Anal. Numér., Vol. 8, pp. 129-151.
- Ciarlet, P. G., 1978, "The finite element method for elliptic problems". North Holland, Amsterdam.
- Franca, L.P. and Frey, S., 1992, "Stabilized finite element methods: II. The incompressible Navier-Stokes equations", Comput. Methods Appl. Mech. Engrg., Vol. 99, pp. 209-233.
- Mitsoulis, E. and Zisis, T., 2001, "Flow of Bingham Plastics in a Lid-Driven Square Cavity", J. Non-Newtonian Fluid Mech., Vol. 101, pp. 173-180.

- Neofytou, P., 2005, "A 3rd order upwind finite volume method for generalised Newtonian fluid flows ", Adv. in Eng. Software, Vol. 36, pp. 664-680.
- Papanastasiou, T.C., 1987, "Flows of materials with yield", J. Rheology, Vol. 31, pp. 385-404.
- Rektorys, K., 1975. "Variational methods in mathematics, science and engineering", D. Reidel Publishing Co.
- Slattery, J. C., 1999, "Advanced Transport Phenomena", Cambridge University Press, U.S.A.
- Zinani, F. and Frey, S., 2006, "Galerkin Least-Squares Finite Element Approximations for Isochoric Flows of Viscoplastic Liquids", Journal of Fluids Engineering – Transactions of the ASME, Vol. 128, pp. 853-863.

8. RESPONSIBILITY NOTICE

The authors are the only responsible for the printed material included in this paper.